

The Effect of Inconel-718 High Strain Rate Sensitivity on Ballistic Impact Response using *MAT_224

Stefano Dolci¹, Kelly Carney¹, Leyu Wang¹, Paul Du Bois¹ and Cing-Dao Kan¹

1Center for Collision Safety and Analysis, George Mason University, Fairfax, VA

Abstract

*A research team from George Mason University, Ohio State University, NASA and FAA has developed material data and analytical modeling that allows for precise input of material data into LS-DYNA® using tabulation and the *MAT_224 material model. The input parameters of this model are based on data from many experimental coupon tests including tension, compression, impact, shear and biaxial stress states. The material model also includes temperature and strain rate effects.*

*The impact physics of Inconel-718 has been incorporated into LS-DYNA using the *MAT_224 material model. Material model failure is based on the results of tests conducted by Ohio State University under many differing states of stress and differing test geometries and on the ballistic impact tests performed by NASA Glenn Research Center. Validation of the set of material constants for this particular alloy, utilizing the tabulated input method of *MAT_224 includes comparisons both to the mechanical property, and ballistic impact tests, with emphasis given to strain rate and temperature effects. The predictive performance of the *MAT_224 material model, including exit velocity and failure mode are evaluated using the test results. It is demonstrated that the strain rate sensitivity of Inconel-718, at strain rates which are currently difficult to obtain in mechanical property tests, has a significant effect on ballistic impact predictions.*

**MAT_224 is an elastic-plastic material with arbitrary stress versus strain curve(s) and arbitrary strain rate dependency, all of which can be defined by the user. Thermo-mechanical and comprehensive plastic failure criterion can also be defined for the material. This requires a process of test data reduction, stability checks, and smoothness checks to insure the model input can reliably produce repeatable results. Desired curves are smooth and convex in the plastic region of the stress strain curves.*



Introduction

The impact physics of Inconel-718 has been incorporated into LS-DYNA using the *MAT_224 material model. Failure in the material model is based on the results of tests conducted by Ohio State University [5][21] under many differing states of stress, differing test geometries, and on the ballistic impact tests performed by NASA Glenn Research Center [2]. Validation of the set of material constants for this particular alloy utilizing the tabulated input method of *MAT_224 includes comparisons both to the mechanical property, and ballistic impact tests, with emphasis given to strain rate and temperature effects. The predictive performance of the *MAT_224 material model, including exit velocity and failure mode are evaluated using the test results. While developing the failure characteristics of Inconel-718, it was found that the strain rate sensitivity of Inconel-718 at higher strain rates [16] was having a significant effect on predicted penetration velocities. This high rate behavior is difficult to obtain in mechanical property tests. Further investigations proved that the strain rate sensitivity of Inconel-718, at high strain rates, referred to as Region IV [14], not only has a significant effect on penetration velocities, but also on the ability to replicate the physical failure mechanisms.

Behavior of Metals at High Strain Rate, Current

Literature Review

A critical aspect in obtaining a representative analysis of ballistic impacts is to include the material behavior at a very high strain rate. Currently, this is a region where it is difficult to measure the properties experimentally. As such there is controversy as to the nature of the material behavior physics. In addition, as this published test data is limited, there is further disagreement in the field as to the real nature of the general behavior of metals at strain rates of 10^4 s^{-1} and greater [8]. Here we present an extensive literature review of high strain rate metal behavior from Carney, et al [8].

Campbell and Ferguson [14] found that the shear strength of a mild steel, is dependent on strain rate as follows: low strain rate, Region I being characterized by a small, nearly constant increase in strength with the logarithm of shear strain rate; Region II where the increase is still constant with the logarithm of the strain rate, but the rate dependence is considerably higher; and Region IV, corresponding to strain rates of greater than $5 \times 10^3 \text{ s}^{-1}$ where the increase in shear strength is directly proportional to the strain rate. Figure 1, showing these regions, is reprinted from [14]. The authors identify Region I as being dominated by long-range internal stresses due to dislocations, precipitate particles, and grain boundaries. Region II is identified as being controlled by the thermal activation of dislocation motion, and Region IV being governed by short-range barriers in combination with an additional dissipative mechanism, but failure not a function of temperature. It is also shown that almost identical strain rate sensitivity behavior for room temperature steel is obtained from dynamic punching, using data from Dowling and Harding [15], and tension, using data from Campbell and Cooper [20], as that from shear loading.

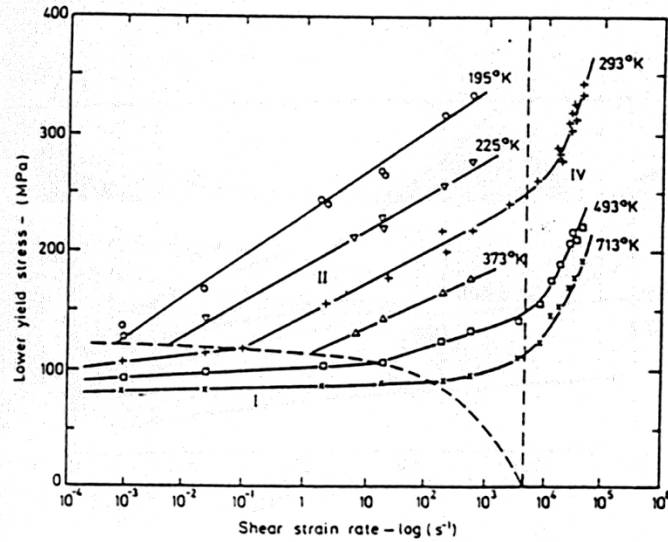


Figure 1: Variation of lower yield stress with strain rate, at constant temperature. From Ref. [14].

Dowling, Harding, and Campbell extended the work on mild steel in reference [22] to aluminum, copper, and brass in reference [15]. The dynamic punch loading of all four of these materials showed the same general strain rate sensitivity as the mild steel in shear of reference [14]. At room temperature, for all four of these materials, there was a small increase in strength, proportional to the logarithm of strain rate, at rates below 10^{-1} s^{-1} , greater increase in sensitivity at rates between 10^{-1} s^{-1} and 10^3 s^{-1} , and at rates above 10^3 s^{-1} even greater sensitivity with the increase being proportional to the strain rate. While the general behavior of the four metals is shown to be similar, the strain rate sensitivity of the four metals is not identical.

Lesuer [17], compiled the stress strain rate response of Ti-6Al-4V titanium alloy from the available literature, and included some additional test data. Very high strain rate data at rates greater than 10^3 s^{-1} was included from Wulf [23] and Meyer [24]. This data shows titanium exhibiting the same shift documented by Dowling, et al, [15] for the other metals. When strain rates exceed approximately $5 \times 10^3 \text{ s}^{-1}$, the strain rate sensitivity becomes a function of the strain rate. However, while at strain rates lower than $5 \times 10^3 \text{ s}^{-1}$, it is a function of the logarithm of the strain rate. Fig. 9 demonstrates this behavior [17]. Wulf [23] also shows that the strain rate sensitivity is not constant.

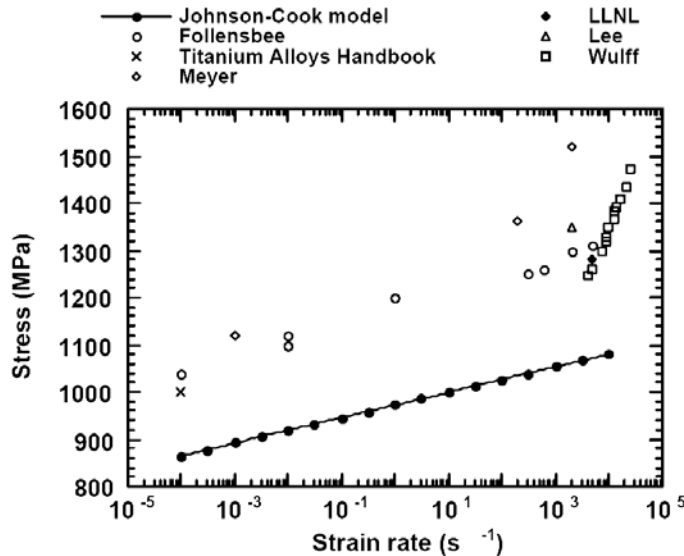


Figure 2: Comparison of the stress-strain rate response of Ti-6Al-4V alloy obtained from this study as well as other studies from the literature. From Ref [17].

Frost and Ashby [25] present a strain-rate map for titanium, which shows the mechanisms responsible for the various failure behaviors. This map associates room temperature failure in Regions I and II with obstacle-controlled plasticity, and failure in Region IV with adiabatic shear.

In review articles Field, et al, [26],[27] present a summary of high rate testing, and discuss using miniaturized Hopkinson bars to obtain strain rates on the order of 10^5 s^{-1} . They also note the increase in strain rate sensitivity at rates $5 \times 10^3 \text{ s}^{-1}$ and higher and concur with Gorham's explanation that it is an artifact of the test configuration [30][31][32]. However, they point out that some non-compression tests, where inertia should not be a factor, also show this phenomenon.

In another review article by Jia and Ramesh [19], the use of miniaturization of the Split-Hopkinson Pressure Bar to obtain stress-strain behavior at strain rates of up to $5 \times 10^4 \text{ s}^{-1}$ is assessed in detail and applied to 6061-T651 aluminum. Comparing the presented strain rate sensitivity at strain rates greater than 10^3 s^{-1} with published quasi-static values of this particular alloy appear to show an increase in strain rate sensitivity, but not to the extent shown in Figure 1 and Figure 2. The authors also state that the explanations of the dramatic increases are occasionally controversial.

Dioh, et al, [28] present analytical and numerical evidence which shows that the apparent increase in the strain rate sensitivity reported in the literature may result from stress wave propagation effects present in the test. Oosterkamp, et al, [29] tested Aluminum Alloys 6082 and 7108 and found that for these alloys, the sudden change in the strain rate sensitivity is a testing artifact. Nemat-Nasser, et al, [18] show that there is a dramatic increase in strain rate sensitivity at approximately $5 \times 10^3 \text{ s}^{-1}$ in a NiTi alloy. They compare images of the failed material at low and high strain rates, demonstrating a different failure mechanism.

In summary, there is disagreement in both the qualitative and quantitative nature of strain rate sensitivity in metals at strain rates greater than approximately 10^5 s^{-1} . While there is uncertainty to the degree to which the strain rate sensitivity slope increase is caused by material or structural response, there is significant evidence that there is a change in the response of metals at strain rates of approximately 10^5 s^{-1} and greater.

*MAT_224 Titanium Alloy

Haight et al, characterized a Ti-6Al-4V alloy for *MAT_224 [12]. The material strain rate sensitivity at high strain rates was extrapolated from the available data (Figure 3). The data available in this study to measure the strain rate sensitivity were up to 10^3 s^{-1} . Therefore, the material behavior at strain rate higher than 10^3 s^{-1} was deduced using a linear extrapolation in Region IV. The ballistic impact simulation obtained with this extrapolation method, showed a good match with ballistic tests as shown in Figure 4.

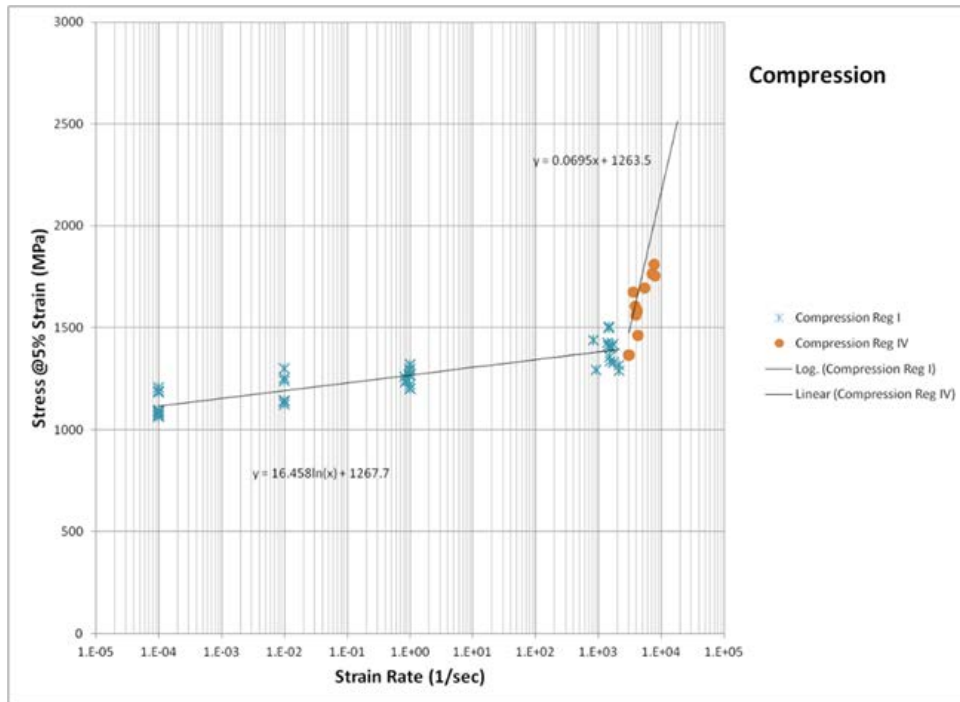


Figure 3: Ti Stress at 5% Strain – Compression Tests. From Ref.[12]

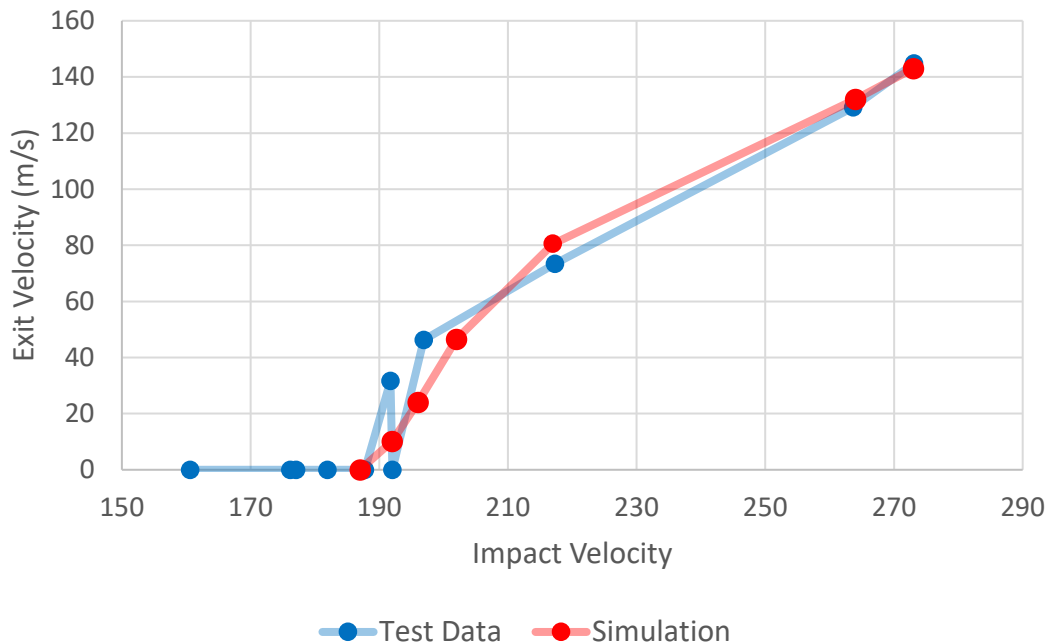


Figure 4: Test Data (blue) and Simulation (red) Results for Ballistic Impact Tests. From Ref.[12]

Previous work on Inconel-718

Failure Model Creation by Simulation of Mechanical Property Tests

The input for *MAT_224 consists of 6 tables to describe strain rate sensitivity and failure characteristics. The creation of the strain rate sensitivity table (tabk1) and temperature sensitivity table (tabkt) for Inconel-718

```
*KEYWORD
*MAT_TABULATED_JOHNSON_COOK_TITLE
Inco-718
$#      mid      ro      e      pr      cp      tr      beta      numint
      3      8.19E-6 210.00000 0.290000      435      300 0.800000 1.000000
$#  tabk1      tabkt      lcf      lcg      lch      lci
      1          2          500      600      700      900
```

Figure 5: Input deck card *MAT_224, Inconel-718

material is described in [16]. Using as starting point the strain rate sensitivity table (tabk1) and temperature sensitivity table (tabkt) from [16], the *MAT_224 input was completed with the remaining tables, enabling the modeling of high velocity impact failures.

First, the tabulated failure surface (lcf) was required. In order to create an effective failure surface, many different tests using different geometries that produce varying states of stress were completed. These tests vary in both triaxiality and Lode Parameter at the localization point or the point of failure (Figure 6). The mechanical property tests were performed by Ohio State University [5][21], who provided the specimen geometry, force data, displacement data, strain data, and DIC images. In total, 22 different specimens were used to determine the failure surface model (Figure 7). These 22 specimens are listed below (with abbreviations):

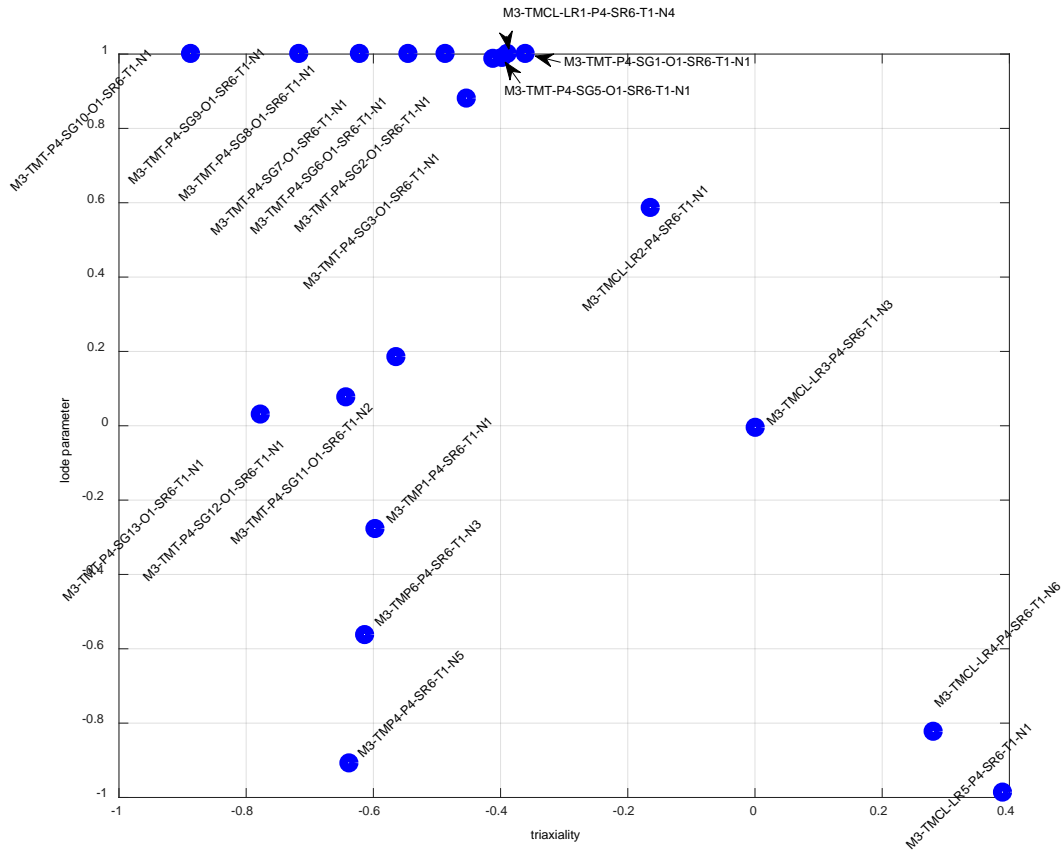


Figure 6: Inconel-718, Tests triaxiality vs Lode Parameter

- SG1: Plane stress specimen (pure tension)
- SG2: Plane stress specimen
- SG3: Plane stress specimen
- SG4: Plane stress specimen
- SG5: Axisymmetric specimen (pure tension)
- SG6: Axisymmetric specimen
- SG7: Axisymmetric specimen
- SG8: Axisymmetric specimen
- SG9: Axisymmetric specimen
- SG10: Axisymmetric specimen
- SG11: Plane strain specimen
- SG12: Plane strain specimen
- SG13: Plane strain specimen
- LR1: Combined (tension/torsion) specimen
- LR2: Combined (tension/torsion) specimen
- LR3: Torsion specimen
- LR4: Combined (compression/torsion) specimen
- LR5: Combined (compression/torsion) specimen
- Punch1: Large diameter punch specimen
- Punch2: Large diameter punch specimen
- Punch3: Large diameter punch specimen
- Compression: Uniaxial (cylindrical) compression specimen

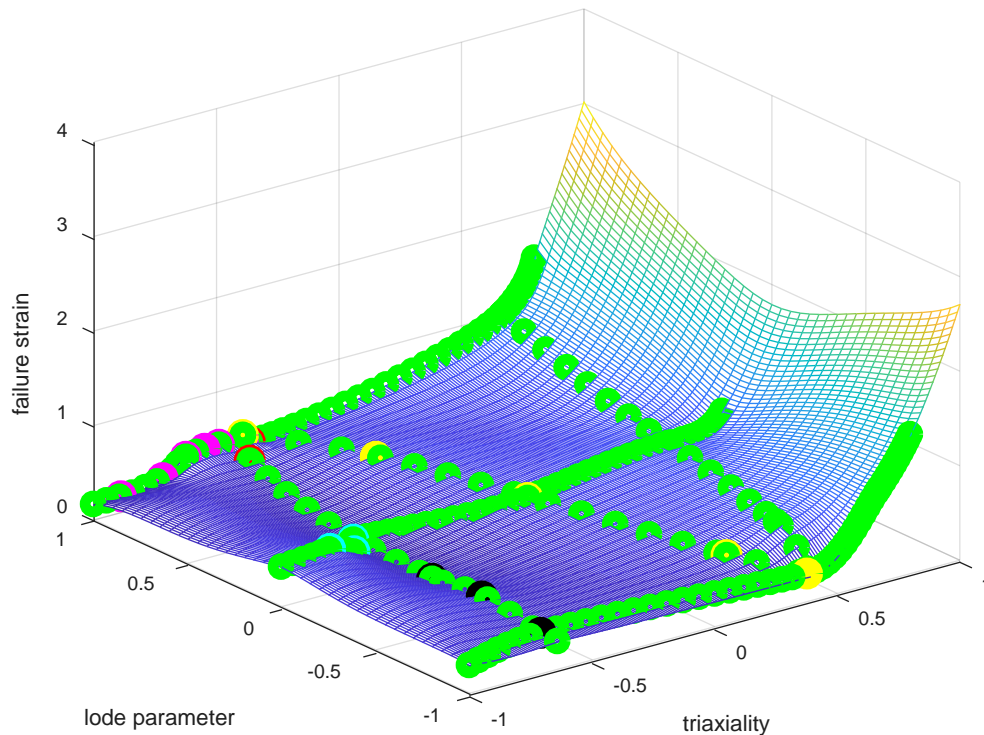


Figure 7: Inconel-718, Failure Surface Generated Using Initial Data Set

The second component which defines the *MAT_224 failure model is the element erosion temperature scaling function (lch). This function is a scaling factor for the failure surface that is dependent on the temperature of the element. For the Inconel-718, five different temperatures were tested: 300 K, 473 K, 673 K, 873 K, and 1073 K. For each temperature, the pure tension plane stress (SG1) specimen was used. It is important to note, that unlike many other alloys, reference [21] shows Inconel-718 gets more brittle at elevated temperatures (around 800 °C). Similarly, an element erosion scaling function was also created for different strain rates (lcr). This scaling function allows the material model to scale the failure surface as a function of the elemental strain rate.

Each of these strain rate tests were simulated using the same procedure as the original SG1 simulation [16]; however here the full material model (strain rate curves, temperature curves, failure surface, temperature scaling curve) was used. This means that these rate dependent tests are modeled including all rate and heating effects. The final component of the Inconel-718 *MAT_224 material model inputs is a mesh size regularization scaling function for element erosion (lci). The mesh size regularization scaling function is critical because element erosion simulations do not converge as the mesh size is reduced [11]. This load curve defines the plastic failure strain as a function of the element size. The element size is calculated by the square root of the volume over the maximum area. The regularization curve is developed by simulating the tension (SG1) specimen with varying mesh sizes. Originally, the mesh size for all the specimens was 0.2 mm. Each specimen was re-meshed with 0.1 mm and 0.4 mm elements, and a scaling function was created for these sizes.

New Inconel-718 high strain rate models

The material sensitivity at high strain rate (Region IV) developed in [16] was used with the failure surface and failure scaling curves developed as reported in the previous section. While simulating the ballistic impact tests performed by NASA Glenn Research Center, the results obtained did not show the correct ballistic limit, nor the physical mechanism of failure. The 0.5" Inconel-718 plates, for the impact speeds tested, present a failure mechanism known as adiabatic shear band. The initial simulations, performed with *MAT_224 characterized in [16] showed a mechanism of crushing-like failure.

Too low of a strain rate sensitivity at high rates was identified as a main cause of this crushing-like failure mode. Three different extrapolations for the material strain rate sensitivity were compared. The first is the original linear extrapolation of Region IV from [16], the second one is still a linear extrapolation of Region IV but with a much higher gradient, and the last one is an extrapolation where the strain rate effects above 10^3 s^{-1} are saturated (see Figure 8). All three of the different extrapolations share the same Region I and Region II, which is crucial to match the material characterization tests. All three of the different extrapolations match the material characterization tests.

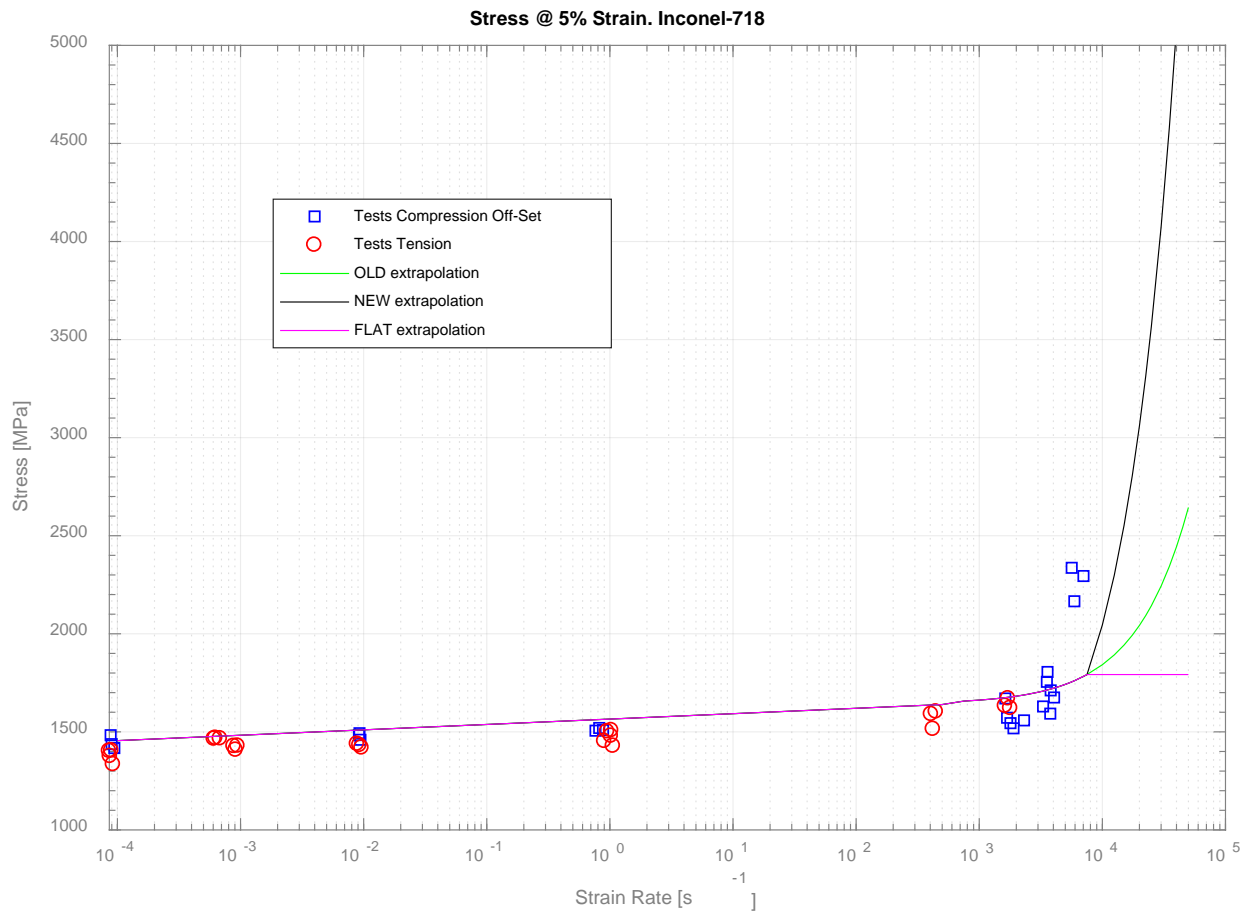


Figure 8: Strain Rate sensitivity extrapolations above 10^3 s^{-1}

Inconel-718 Current Results

The current results (Table 1 ,Table 2) from the simulations of the Inconel-718 material model did not accurately predict the ballistic limit (velocity at which penetration occurs) measured by NASA tests (Figure 9). The strain rates in these analyses went up to 35000 s^{-1} , well into Region IV, while the available mechanical property data went up to 10^3 s^{-1} . The predicted ballistic limit is higher than that of the tests, and so element erosion is deficient. The results for both the baseline elastic projectile model described in [12], and a new *MAT224 projectile material model based upon very recent testing of Ohio State University, are presented in Tables 1 and 2.

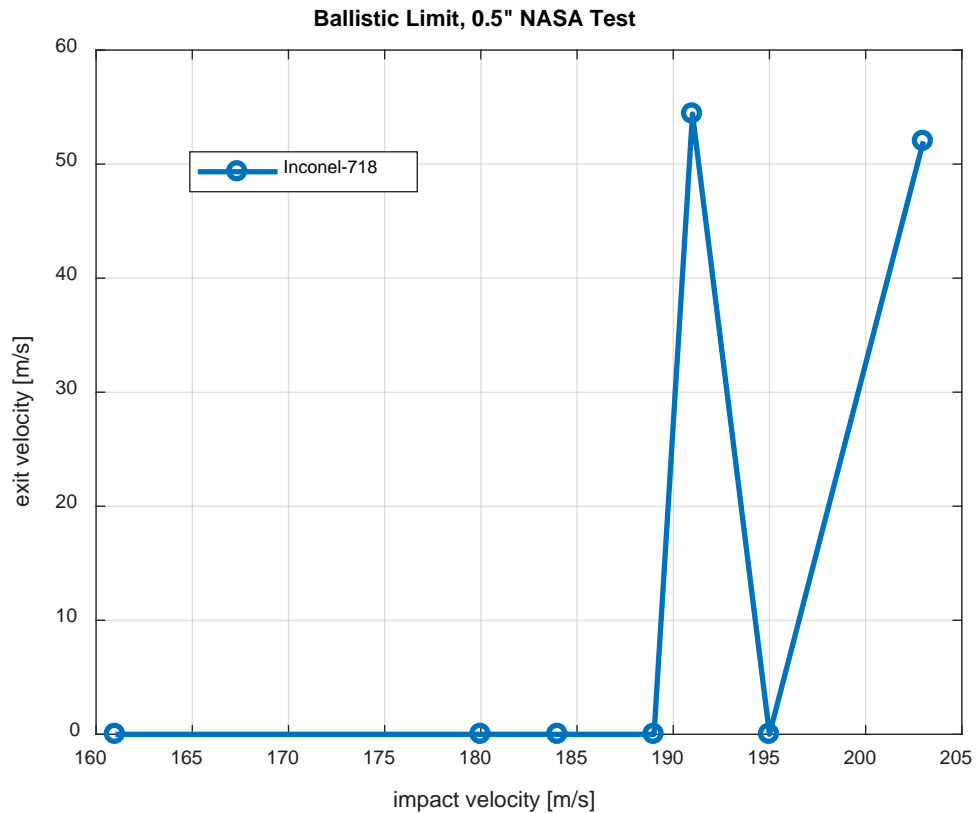


Figure 9: Ballistic limit, Inconel-718 0.5” plate

The most likely reason for insufficient element erosion is that the mesh density is not sufficiently high to capture the adiabatic shear bands' extreme local deformation. Consequently, the analysis does not predict the actual rise in temperatures caused by adiabatic heating in the corresponding elements. It appears that in any case, the simulations presenting the correct failure mechanism (with the initiation of a crack and a plug) are the two with the linear extrapolation in Region IV. The shear band begins to form but does not open fully. It should also be noted that the analysis with the stronger gradient in the extrapolated Region IV predicts higher temperatures, above 600K, somewhat closer to the temperatures where Inconel-718 becomes brittle.

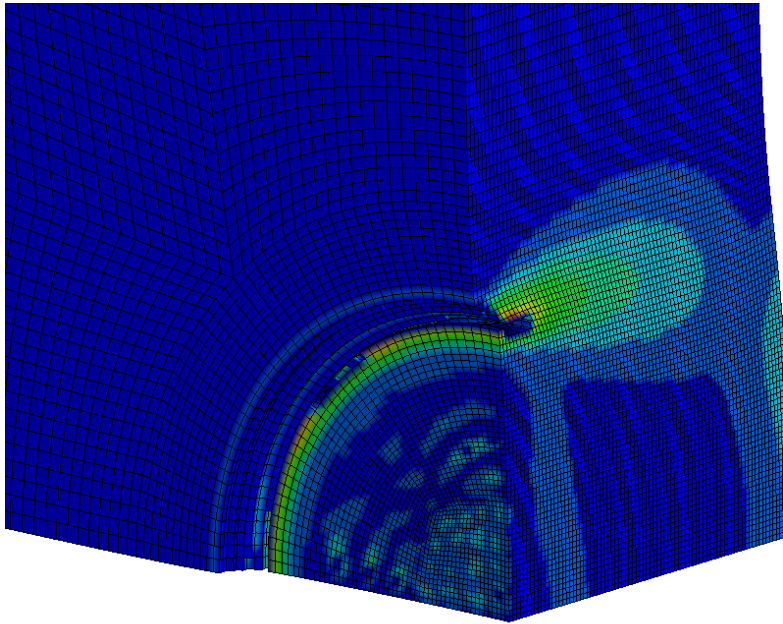
Inconel-718

Projectile *MAT224

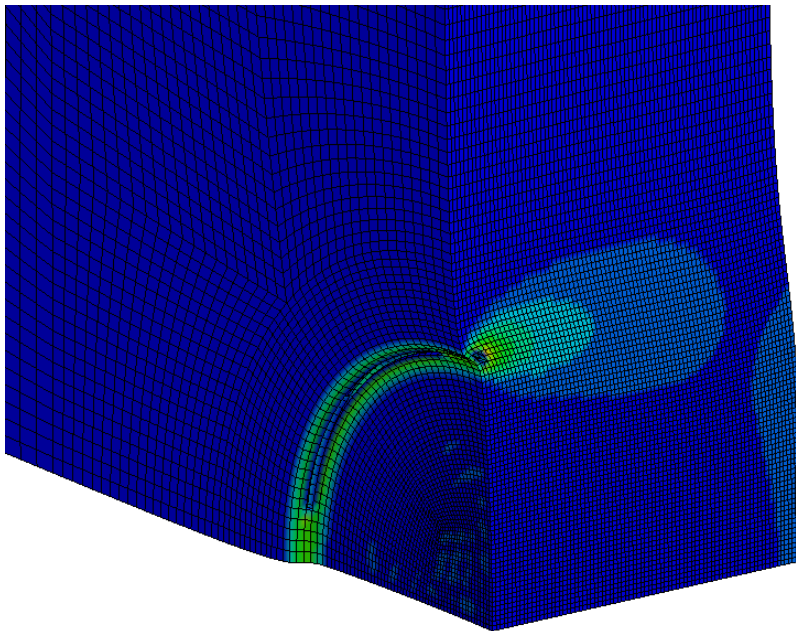
Axisymmetric MESH

203

Low SR
sensitivity
(OLD)



High SR
sensitivity
(NEW)



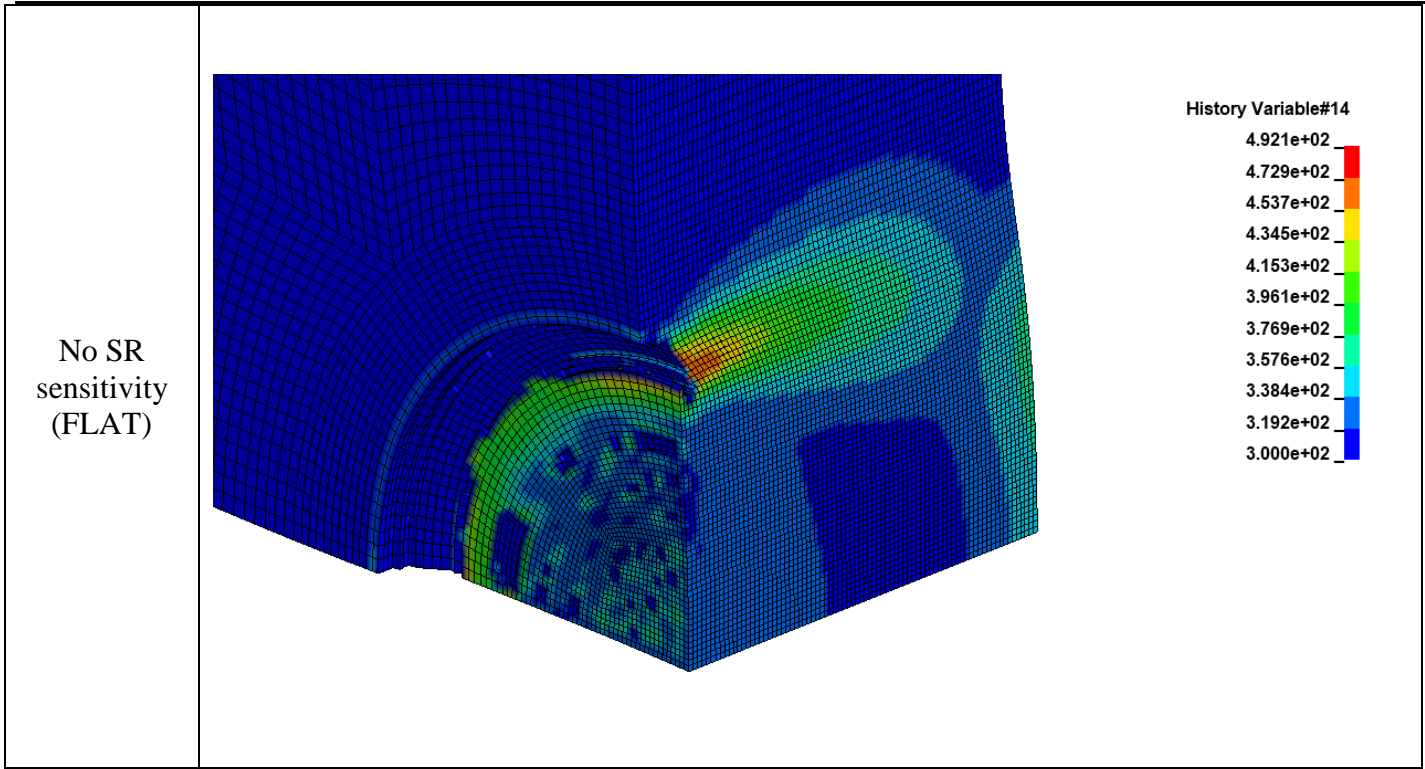
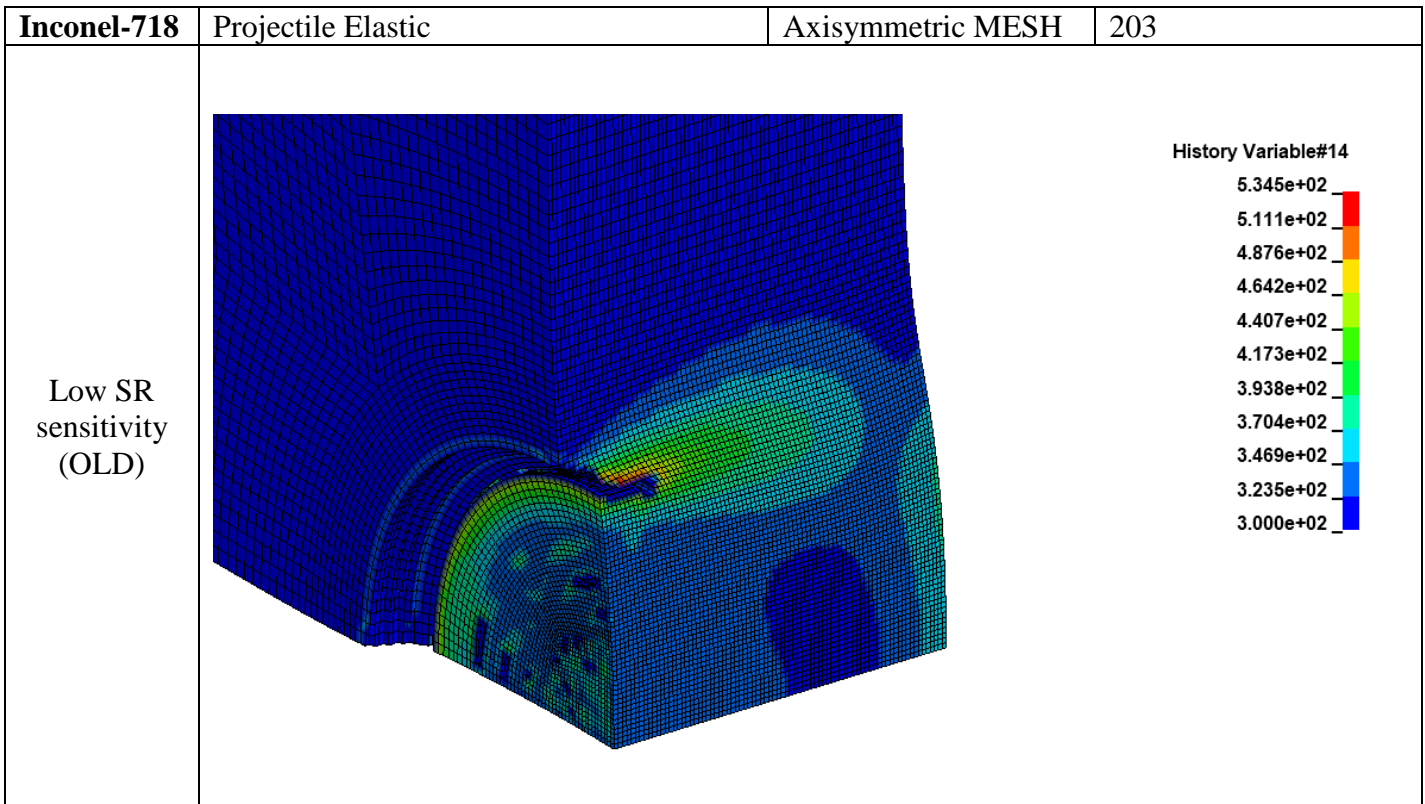


Table 1: Temperature raise in 0.5” Inconel-718 plate. Impact velocity 203 [m/s], 80 elements trough the thickness, *MAT_224 projectile



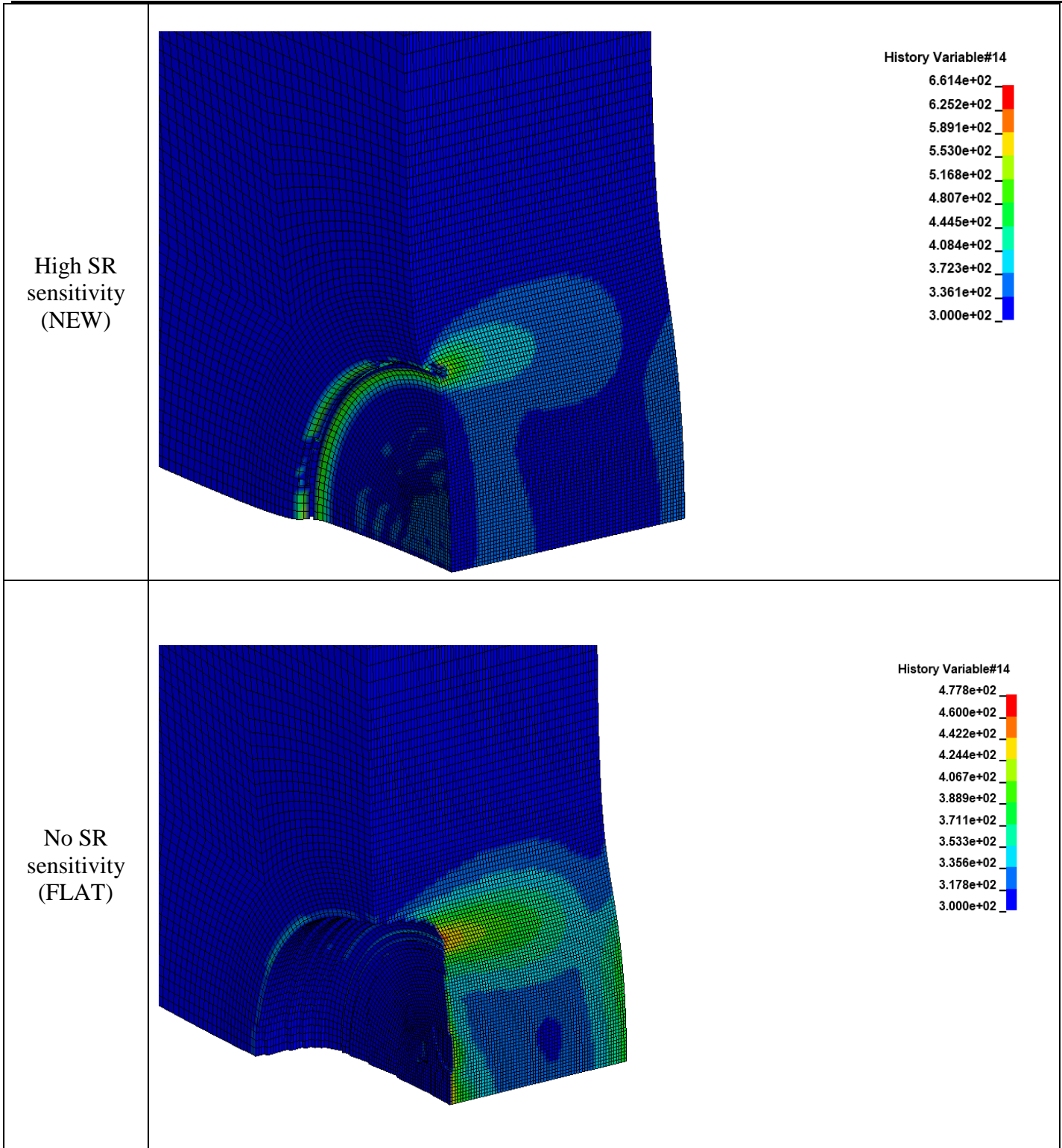


Table 2: Temperature raise in 0.5” Inconel-718 plate. Impact velocity 203 [m/s], 80 elements trough the thickness, elastic projectile

Conclusions

We present evidence that Inconel-718 and Ti6Al4V, have linear stress-strain rate sensitivity at strain rates greater than approximately 10^3 s^{-1} caused by material response (Region IV). Modeling this sensitivity accurately is crucial to predict the ballistic limit within a ballistic simulation. Moreover, modeling this behavior accurately allows us to obtain a physical behavioral model consistent with the failure observed in the ballistic tests.

References

- [1] *LS_DYNA Manual*, Version 971, Livermore, CA, 2017.
- [2] Pereira, J. Michael, Revilock, Duane M., Lerch, Bradley A. and Ruggeri, Charles R.; "Impact Testing of Aluminum 2024 and Titanium 6Al-4V for Material Model Development", *Technical Memorandum NASA/TM 2013-217869*, NASA Glenn Research Center, Cleveland, 2013.
- [3] Yatnalkar, Ravi Shriram; "Experimental Investigation of Plastic Deformation of Ti-6Al-4V under Various Loading Conditions", B.E. Thesis, The Ohio State University, 2010. Print.
- [4] Seidt, Jeremy Daniel; "Plastic Deformation and Ductile Fracture of 2024-T351 Aluminum under Various Loading Conditions", Dissertation, The Ohio State University, 2010. Print.
- [5] Ressa, A., Liutkus, T., Seidt, J., Gilat, A., "Time Dependent Response of Inconel-718", *Challenges in Mechanics of Time Dependent Materials, Volume 2* 2015-12.
- [6] "Tensile Strength or Tension Test", *About Civil.Org*, Web. Retrieved 2014-10-28, www.aboutcivil.org/tension-test-tensile-strength-test.html
- [7] "INCONEL-718 TECHNICAL DATA", *High temp Metals*, Web. Retrieved 2016-03-02. <http://www.hightempmetals.com/techdata/hitempInconel718data.php>
- [8] Carney, K., Pereira, M., Revilock D., and Matheny P., "Jet Engine Fan Blade Containment using an Alternate Geometry and the Effect of Very High Strain Rate Material Behavior," *International Journal of Impact Engineering*, 36 (2009) pp 720-728.
- [9] Ravichandran, Rosakis, Hodowany, and Rosakis "On the Conversion of Plastic Work into Heat during High-Strain-Rate Deformation," *Shock Compression of Condensed Matter - 2001*.
- [10] Rosakis, Rosakis, Ravichandran, and Hodowany, "A Thermodynamic Internal Variable Model for the Partition of Plastic Work into Heat and Stored Energy in Metals," *Journal of the Mechanics and Physics of Solids*, 48 (2000) 581-607.
- [11] "AWG Modeling Guidelines Document," **LS-DYNA Aerospace Working Group**, Web. Retrieved 2015-4-28. <http://awg.lstc.com/tiki/tiki-index.php?page=MGD>
- [12] Sean Haight, Leyu Wang, Paul Du Bois, Kelly Carney, Cing-Dao Kan "Development of a Titanium Alloy Ti-6Al-4V Material Model Used in **LS-DYNA**" DOT/FAA Report 2015-05-26.
- [13] Hammer, Jeremiah Thomas; "Plastic Deformation and Ductile Fracture of Ti-6Al-4V under Various Loading Conditions", M.S. Thesis, The Ohio State University, 2012. Print.
- [14] J.D. Campbell, W.G. Ferguson, "The Temperature and Strain-Rate Dependence of Shear Strength of Mild Steel. The Philosophical Magazine: A Journal of Theoretical Experimental and Applied Physics_Vol. 21, Iss. 169, 1970
- [15] A.R. Dowling, J. Harding, J.D. Campbell, "The Dynamic Punching of Metals". *Journal of Institute of Metals*, 98 (1970) 215-224.
- [16] Stefano Dolci, Kelly Carney, Leyu Wang, Paul Du Bois and Cing-Dao Kan, "Incorporation of Inconel-718 material test data into material model input parameters for *MAT_224" 14th International LS-DYNA Users Conference.
- [17] Lesuer DR. Experimental investigations of material models for Ti-6Al-4V Titanium and 2024-T3 Aluminum. DOT/FAA/AR-00/25; 2000.
- [18] Nemat-Nasser S, Choi JY, Guo WG, Isaacs JB. Very high strain-rate response of a NiTi shape-memory alloy. *Mech Mater* 2005;37:287-98
- [19] Jia D, Ramesh KT. A rigorous assessment of the benefits of miniaturization in the Kolsky bar system. *Exp Mech* 2004;44(5).
- [20] Campbell JD, Cooper RH. Physical basis of yield and fracture. London: Institute of Physics and Physical Society; 1966. p. 77.
- [21] Ressa, A. "Plastic Deformation and Ductile Fracture Behavior of Inconel 718", 2015, Master of Science, Ohio State University, Mechanical Engineering
- [22] Dowling AR, Harding J. In: First International Conference of Center for HighEnergy Forming, vol. 2. Denver, CO, USA: University of Denver; 1967. 7.3.1.
- [23] Wulf GL. High-strain rate compression of titanium and some titanium alloys. *Int J Mech Sci* 1979;21:713-8.
- [24] Meyer LW. Strength and ductility of a titanium-Alloy Ti-6Al-4V in tensile and compressive loading under low, medium and high rates of strain. *Titanium Sci Technol* 1984:1851-8.
- [25] Frost HJ, Ashby MF. Deformation-mechanism maps, the plasticity and creep of metals and ceramics. New York: Pergamon Press; 1982.
- [26] Field JE, Walley SM, Proud WG, Goldrein HT, Siviour CR. Review of experimental techniques for high rate deformation and shock studies. *Int J Impact Eng* 2004;30:725-75.
- [27] Field JE, Walley SM, Bourne NK, Huntley JM. Review of experimental techniques for high rate deformation studies. In: Proceedings of the Acoustics and Vibration Asia 98 conference, Singapore; 1998. p. 9-38.
- [28] Dioh NN, Ivankovic A, Leever PS, Williams JG. Stress wave propagation effects in split Hopkinson pressure bar tests. *Proc Math Phys Sci* 1936;449:187-204.

- [29] Oosterkamp LD, Ivankovic A, Venizelos G. High strain rate properties of selected aluminum alloy. *Mater Sci Eng* 2000;278:225–35.
- [30] Gorham DA. The effect of specimen dimensions on high strain rate compression measurements of copper. *J Phys D* 1991;24:1489–92.
- [31] Gorham DA, Pope PH, Field JE. An improved method for compressive stress -strain measurements at very high strain rates. *Proc R Soc Lond A* 1992; 438:153–70.
- [32] Gorham DA. Specimen inertia in high strainrate compression. *J PhysAppl Phys* 1989;22:1888–93.

Acknowledgments

The authors would like to thank the Federal Aviation Administration of the U.S. Department of Transportation for their support of this research.